Bull. Mater. Sci. (2021)44:126
https://doi.org/10.1007/s12034-021-02425-2

Thymol-functionalized hollow mesoporous silica spheres nanoparticles: preparation, characterization and bactericidal activity

YUHAO LIU[1], LI JIN[1], CHEN WANG[1], JIE SHENG[1] and YISHAN SONG[1,2,*]

[1]College of Food Science and Technology, Shanghai Ocean University, Shanghai 201306, China
[2]College of Food Science and Technology, Laboratory of Quality and Safety Risk Assessment for Aquatic Products on Storage and Preservation (Shanghai), Ministry of Agriculture and Shanghai Engineering Research Center of Aquatic-Product Processing and Preservation, Shanghai Ocean University, Shanghai 201306, China
*Author for correspondence (yssong@shou.edu.cn)

MS received 22 August 2020; accepted 20 January 2021

Abstract. Antimicrobial natural products show good antimicrobial activities; however, some of them have unpleasant odor or high volatility that limits their application in food industry. One of solutions is to introduce them in inorganic media. In this study, hollow mesoporous silica sphere (HS) was used to encapsulate natural organic antimicrobial agent thymol, and antimicrobial activity of the resulted antimicrobial agent (HST) was tested. Materials characterization revealed that the thymol was successfully introduced into the cavities of HS, and the inorganic host exhibited a high loading capacity of 1320 mg g^{-1}. In addition, the antibacterial activities were tested by double-fold dilution method, the minimum bactericidal concentrations of HST against *Escherichia coli* (*E. coli*) and *Staphylococcus aureus* (*S. aureus*) were decreased compared with that of thymol. Furthermore, scanning electron microscopy observation confirmed that HST indeed showed a notable inhibitory effect against *E. coli* and *S. aureus* by disrupting cell membrane structure.

Keywords. Thymol; hollow mesoporous silica spheres; bactericidal activity.

1. Introduction

Microbial contamination in food not only results in a reduction of a product's shelf life and food deterioration, but can also lead to disease and economic loss, and consumers are increasingly concerned about food safety problems caused by food pathogenic microorganisms. Therefore, antimicrobial agents are used in the food industries and play an important role since they are able to either inhibit the growth or inactivate pathogenic or spoilage microorganisms [1].

Furthermore, natural antimicrobial agents have attracted much attention because of their low toxicity [2–4]. However, the number of compounds allowed by regulations to be used in foods is very limited since natural antimicrobial agents usually show high volatility, strong sensory property and instability [5,6]. To overcome these disadvantages, it is necessary to adopt some novel strategies, including the utilization of nanotechnologies [7–9], to improve the physicochemical properties of natural antimicrobial agents and meantime still maintain/enhance their bioactivities [10]. A large number of experimental studies have been developed to improve natural antimicrobial agents' function by nanotechnologies [11–15].

Recently, mesoporous silica materials such as MCM-41 and SBA-15 have widely been used in food system because of their nontoxic nature, tunable pore diameter, large surface area, high thermal stability and controllable structures [16–19]. However, their storage capacity is relatively low, and the irregular bulk morphology is not perfect for delivery [20–23]. As the most promising nanoloading system for smart delivery, hollow mesoporous silica spheres (HS) have attracted considerable interest in the past few decades due to their well-defined morphology, on the nanoscale with pore channels penetrating from the outside to the inner hollow core, favourable for the target molecular adsorption and release [24–26]. However, to our best knowledge, there is no report about the application of HS in construction of antimicrobial agents.

Herein, in this study, thymol-functionalized HS were prepared, thymol was selected because it widely exists in plants, has good antimicrobial abilities and unpleasant odour [27]. The structure of the resulted antimicrobial agent (HST) was characterized, and the antibacterial activities were tested. The results indicated that HS has high loading capacity and can enhance the bactericidal activity of thymol. This research is of great significance in the synthesis of

Published online: 30 April 2021

a novel kind of antimicrobial agent, and potential for food preservation.

2. Materials and methods

2.1 *Materials*

Thymol, tetraethyl orthosilicate (TEOS, 98%), aqueous ammonia (28%), cetyltrimethylammonium bromide (CTAB), absolute ethanol (99.8%), hydroxide (NaOH, 99%), hydrochloric acid (HCl, 37%), sodium chloride (NaCl, 99%), *n*-hexane, phosphate buffer saline (PBS, 0.1 M, pH = 7.4) and glutaraldehyde (25%) were all of analytical grade and provided by Sangon Biotech (Shanghai, P. R. China).

2.2 *Synthesis of HS*

The synthesis procedure of HS was listed according to previously described protocol [28] with some modifications: 0.15 g CTAB was dispersed in 74 ml of ethanol–water mixture and vigorously stirred for 2 h. Subsequently, ammonium hydroxide (0.25 ml, 25 wt%) was added dropwise to the mixed solution, followed by addition of 1 ml of TEOS. Stirring was continued for 24 h at room temperature, and then the precipitates were separated by centrifugation at 4000 rpm for 15 min and washed three times with deionized water. Thereafter, the samples were dispersed into deionized water (240 ml) and kept at 70°C for 2 h. The white as-prepared materials were collected by centrifugation, and washed with ethanol. Finally, the obtained silica nanoparticles were calcined at 550°C for 4 h at a heating rate of 1°C min^{-1} to remove the surfactant CTAB.

2.3 *Preparation of HST*

The formation of thymol-functionalized hollow mesoporous silica spheres (HST) was started by weighting 200 mg of pure particles (HS) into a round-bottomed flask with an inert atmosphere. Later, 200 mg of thymol solution in ethanol with concentration of 20 mg ml^{-1} was added and stirred for 24 h at room temperature to maximize loading of the thymol into the hollow spheres. Finally, the mixture was filtered by vacuum filtration, and the solids left were dried at room temperature for 24 h.

2.4 *Characterization*

The chemical characterizations of the HS and HST were conducted by standard techniques, including field emission-scanning electron microscope, Fourier transform infrared (FT-IR) spectroscopy and Brunauer-Emmett-Teller.

The morphological structures of HS and HST were observed by field emission-scanning electron microscope (Hitachi S-4800, Japan). Briefly, about 10 mg of HS and HST were dispersed in double-sided copper conductive tape. The samples were coated with gold for 90 s, and the images were obtained on a field emission-scanning electron microscope at an accelerating voltage of 3 kV.

The FT-IR spectra (Nicolet Instrument, Thermo Company, USA) were recorded to analyse the chemical composition of thymol, HS and HST at 25°C. A small amount of samples were respectively covered onto the surface of the ATR diamond and pressed by the clamp with constant pressure. Each 64 scans of the spectra were measured in transmittance mode within 500–4000 cm^{-1} wavenumber's range at a resolution of 4 cm^{-1}.

2.5 *Strains and growth conditions*

The *Escherichia coli* (*E. coli*) ATCC 25992 (Gram-negative) and *Staphylococcus aureus* (*S. aureus*) ATCC 25923 (Gram-positive) were obtained from Shanghai Ocean University, P. R. China. All strains were stored at 4°C in tryptic soy agar (TSA) before use. The cells from a colony grown on TSA were transferred to 10 ml of tryptic soy broth (TSB) and incubated at 37°C for 24 h to obtain an inoculum density of approximately 10^8 CFU ml^{-1} of broth for testing.

2.6 *Antimicrobial activity of thymol*

The double dilutions method was used to determine the minimum bactericidal concentration (MBC) of thymol [29]. Firstly, different amounts of thymol was dissolved in 35% ethanol to obtain the different concentrations. Next 100 µl of the prepared thymol solution was added to the first well of the 96-well plate and mixed with 100 µl of TSB. Serial double dilutions were performed by TSB to obtain final concentrations ranging from 0.2 to 3 mg ml^{-1} per well. After performing the double dilutions, 100 µl of microbial suspension, adjusted to an inoculum density of approximately 10^5 CFU ml^{-1}, was added in each well. Finally, the 96-well plate was placed in a constant temperature incubator and cultured at 37°C for 24 and 48 h. The positive control (microtiter plates containing inoculum and nutrient broth) was used to quantify the microbial count in the absence of treatment, and the microtiter plate containing 35% ethanol and nutrient broth was also tested as a negative control. All the treatments were performed in triplicate. After incubation, viable cell numbers were determined as colony-forming units (CFU) by the serial dilution coating method using TSA. These values were logarithmically transformed and expressed as log10 CFU ml^{-1}.

2.7 *Antimicrobial activity of HST*

The antimicrobial activity of the HST was determined similarly with thymol. The equivalent amounts of the HST were calculated according to the results obtained when determining the loading efficiency of thymol. Briefly, the modified nanoparticles were suspended in TSB to obtain different concentrations suspension of 0.2, 0.4, 0.8, 1.6, 3.2 mg ml^{-1} and 0.5, 1, 1.5, 2, 2.5 mg ml^{-1}, respectively. The strains of *E. coil* and *S. aureus* were appropriately diluted to reach a density of approximately 10^6 cells ml^{-1} in TSB. Then test tubes with 10 ml of different concentrations suspension were inoculated with 100 µl of inoculum and incubated at 37°C for 24 and 48 h with orbital stirring (150 rpm). Finally, viable cell numbers of the two groups as CFU was determined by serial dilution coating method. These values are logarithmically converted to log CFU ml^{-1}. All the treatments were performed in triplicate, including positive control (test tube containing inoculum and nutrient solution) and negative control (test tube containing HS and nutrient solution).

2.8 *The mechanism of antibacterial*

In order to further explore the mechanism of antibacterial, the morphological changes of cells were observed by scanning electron microscopy (SEM). Different concentrations of HST were inoculated to the strain of *E. coil* and *S. aureus*, and incubated at 37°C with orbital stirring for 24 h. After centrifugation at 4000 r for 10 min, the bacterial suspension was fixed with 2.5% glutaraldehyde for 10 h, and then washed twice with 0.1 M Phosphate-buffered saline solution. After gradient dehydration in 30, 50, 70, 90 100% ethanol solution, the cells were freeze-dried for 24 h. Finally, the morphological changes of cells were observed under SEM.

3. Results and discussion

3.1 *FT-IR spectroscopy*

Figure 1 presented the FT-IR spectra of HS (a), HST (b) and thymol (c). For HS, the curve exhibits the characteristic peak of Si–O–Si group at 1047 cm^{-1}, and the weak peaks at ~2920 and ~2853 cm^{-1} are attributed to asymmetric stretching of CH_2 group of CTAB and C–H in the hollow spheres structure. For thymol, the peak at 3354 cm^{-1} is due to stretching vibration of –OH group, the peak at 2951 cm^{-1} are attributed to stretching vibration of $–CH_3$ group from benzene ring, and peaks range at 1418–1642 cm^{-1} can be assigned as stretching vibration of C=C from benzene ring.

Compared with thymol, HST showed similar infrared absorption bands at the range 1421–3358 cm^{-1}, indicating that the organic component was embedded onto the wall of hollow spheres. In addition, the absorption band at 1057 cm^{-1} was overlapped by the absorption band of the Si–O–Si bonds in the 1046 cm^{-1}. The results imply that thymol functionalized HS nanoparticles successfully.

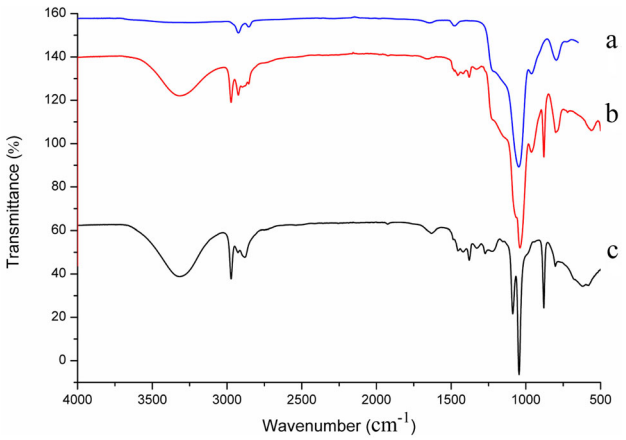

Figure 1. FT-IR spectra of (**a**) HS, (**b**) HST and (**c**) thymol.

3.2 *Thymol loading study*

The loading properties of hollow spheres were explored using UV-viz detector by the standard curve ($y = 0.0203x + 0.0049$, $R^2 = 0.9946$), and the absorbance of thymol and HST were measured at 292 nm. As a result, the inorganic host exhibited a high loading capacity of 1320 mg g^{-1}. The high loading capacity is mainly attributed to the large pore volume of hollow spheres.

3.3 *N_2 adsorption–desorption isotherm*

Figure 2 shows the N_2 adsorption–desorption isotherm for HS and HST. The two curves are similar and display type IV isotherms with H1-type hysteresis loops at high relative pressures in accordance with the IUPAC classification, indicating that they both possess a well-defined structure of regular mesoporous array. In addition, it may be concluded that the introduction of thymol did not destroy the mesoporous structure of the prepared host HS. This is because the concentration of the thymol component in the mesoporous system occupies only few channels of the HS host. The adsorption capacity of HST is weaker than that of HS, meaning HST has lower pore volume, which is further evidence of the presence of thymol component in the channels of HS.

3.4 *Scanning electron microscope*

The size and morphology of HS and HST were determined by SEM images, as shown in figure 3. It can be seen that the size of HS was ~600 nm, with little difference of size

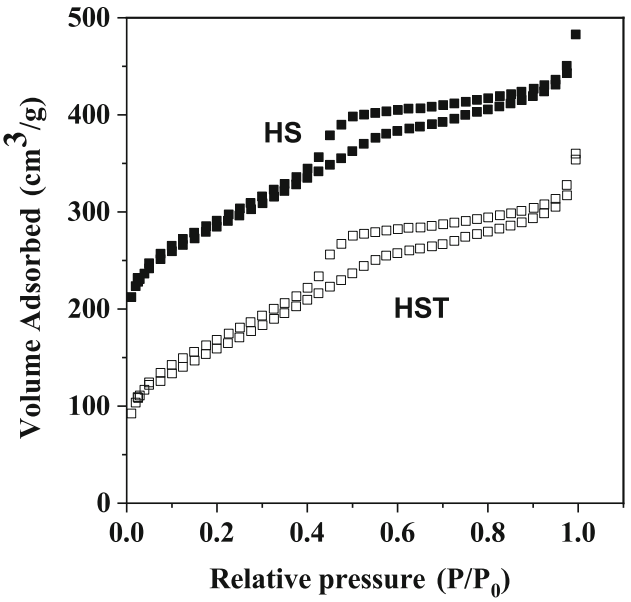

Figure 2. N_2 adsorption–desorption isotherm for HS and HST.

distribution. The reason is that the size of HS is related to the amount of ammonia in the preparation process, under otherwise constant experimental conditions, the particle sizes could be larger with the increase of ammonia hydroxide concentration [28].

Furthermore, HS has the unique and uniform spherical morphology, and HST remains unchanged in loading process. That is the fact for the high stability and strong adsorption of HS.

3.5 *Antimicrobial activity of thymol*

The growth of *E. coil* and *S. aureus* was determined by adding different thymol concentrations, and then the antibacterial and bactericidal activities of thymol were analysed. After observing the turbidity of the mixture in the hole cultured for 24 h on the 96-well plate, it was found that the mixture in the hole with the concentration of 2.5 and 3.2 mg ml^{-1} thymol was clear and transparent, and the hole with the concentration of 1.6 and 2 mg ml^{-1} was turbid, respectively. Therefore, the solution present in the hole with the concentration ranged from 0.2 to 4.8 mg ml^{-1}, cultured for 24 h, and counted the number of colonies on the plate.

It can be seen from figure 4a that the bacterial concentration of *E. coil* original bacterial solution decreases with the increase of thymol concentration, which is the lowest bactericidal concentration (MBC) when the concentration of thymol is 3.2 mg ml^{-1}. Because of the difference of cell membrane structure between Gram-negative and positive bacteria, thymol may have different sensitivity to the antibacterial effect of positive bacteria. It can be seen from figure 4b that the bacteriostatic effect of thymol concentration on *S. aureus* is better than that of *E. coil*, and the minimum bactericidal concentration is 2.5 mg ml^{-1}. With the increase of thymol concentration, the bacteriostatic effect is more and more obvious. There was no significant difference in the bacteriostasis of thymol to Gram-negative bacteria, so the data of 48 h is not shown.

3.6 *Antimicrobial activity of HST*

Figure 4c shows the bacterial concentration changes of *E. coil* after mixed culture with different concentrations of synthetic materials. The growth rates of *E. coil* had a significant inhibitory trend at an increasing concentration gradient. This conclusion showed that the minimum inhibitory concentration (MBC) was 1.6 mg ml^{-1} at 24 and 48 h. With the passage of time, the HST did not reduce the antimicrobial activity of thymol, but increased the bactericidal concentration to *E. coil*. Furthermore, figure 4d shows the change of bacterial concentration after the mixed culture of *S. aureus* and synthetic materials with different concentrations. It could be found that the growth inhibition rate of *S. aureus* is similar with the *E. coil* at different concentrations. These results showed that the antibacterial

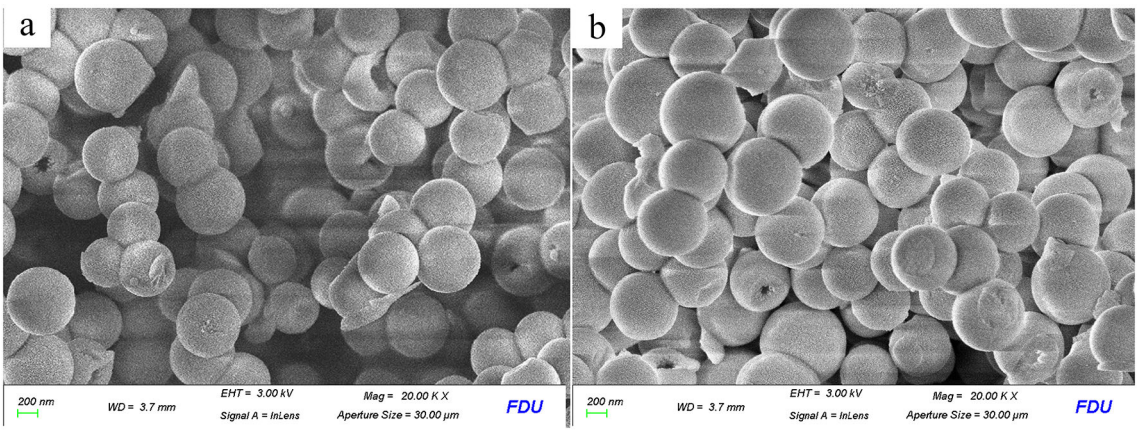

Figure 3. SEM images of the (**a**) HS and (**b**) HST.

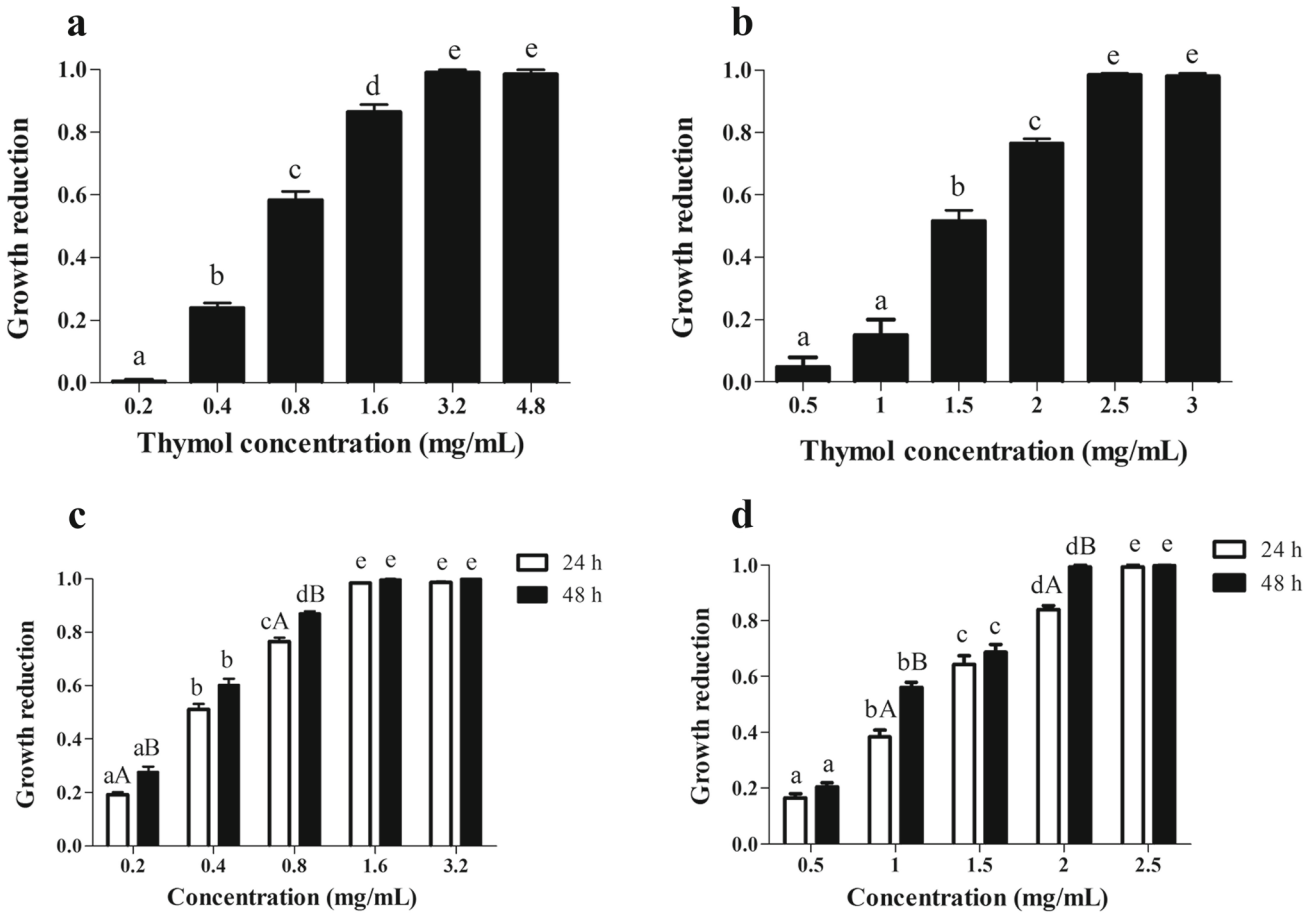

Figure 4. The growth reduction of (**a** and **c**) *E. coli* and (**b** and **d**) *S. aureus* treated with different loading thymol concentrations at 24 and 48 h. Different letters in the bars indicate statistically significant differences ($P < 0.05$) from levels of concentration (small letters) and exposure time (capital letters) ($n = 3$).

effect of the synthetic material was very obvious at the lower concentration of thymol, and even at the concentration of 2 mg ml^{-1} thymol, the mesoporous material of thymol had reached the lowest concentration. In addition, 48 h is better than 24 h, which shows that thymol has a slow-release process in the mesoporous materials, to achieve a better and longer antibacterial effect.

3.7 *The mechanism of antibacterial*

In order to further explore the antibacterial mechanism of functionalized nanoparticles, the morphological changes of *E. coli* and *S. aureus* cells treated with or without HST were studied by SEM. As shown in figure 5a and b, *S. aureus* exhibited an intact cell membrane and cell wall without HST. However, the cell membrane was completely destroyed and cytoplasm was leaked in the presence of HST. Similarly, figure 5c showed the smooth cell wall and complete structure of *E. coli* untreated with HST. After HST treatment, *E. coli* showed a rough surface and damaged cell wall (figure 5d) compared with untreated control.

Obviously, these results indicated that the thymol encapsulated in the hollow spheres lead to the destruction of the cell wall and membrane. It has been reported in previous studies that the mechanism of action of thymol is due to the fact that the hydroxyl group contained in thymol interacts with the cell membrane to affect the membrane permeability, causing the cell membrane to be destroyed and cytoplasm to flow out [30].

Furthermore, HST showed different antibacterial activity against *E. coli* and *S. aureus*, which may be due to the differences of the complexity of the cellular wall of the Gram-positive and Gram-negative bacterial cells [31]. Other studies have suggested that the existence of specific interactions between the nanoparticles and the bacterial cell wall may influence the bactericidal activity of the delivered drug [32]. The loading drugs are even more effective than the drug in solution because interaction with a nanoparticle loaded with drugs will expose a bacterial cell to a high local concentration of the drug that more effectively results in perforation of the cell membrane [33]. The drugs are absorbed onto the surface of bacteria and greater the surface area of bacteria the

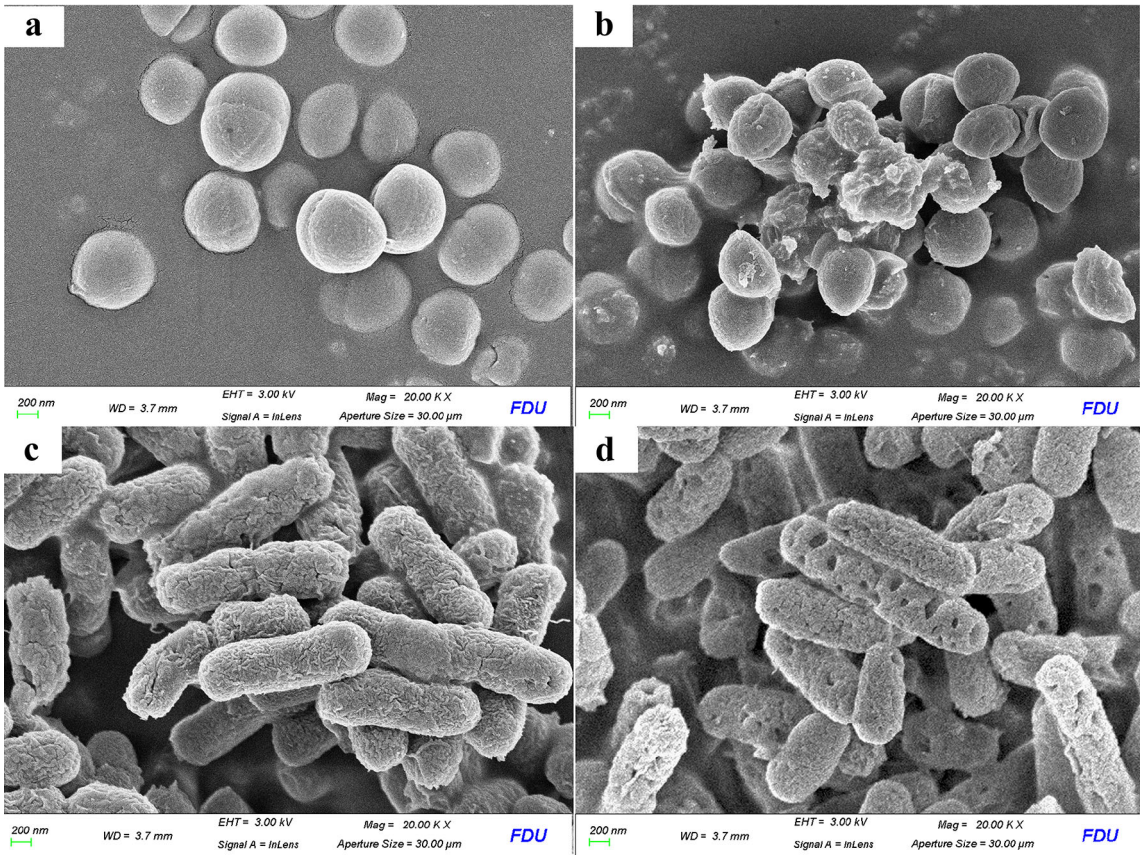

Figure 5. SEM images of (**a** and **b**) *E. coil* and (**c** and **d**) *S. aureus* untreated and treated with HST for 24 h.

stronger inhibitory effect [34]. Compared with *E. coli* cells, *S. aureus* cells are spherical and smaller, which increased their specific surface area. Therefore, the larger specific surface area of *S. aureus* makes it strongly inhibited, which may be one of the reasons for the different inhibitory activity of HST against *E. coli* and *S. aureus.*

4. Conclusion

In this study, HS with stable structure was synthesized, and thymol as natural organic antimicrobial agent was encapsulated in the HS to prepare novel antibacterial agent. HST was characterized by SEM, FT-IR and Brunauer-Emmett-Teller, and the results indicated that HS was successfully functionalized and exhibited good stability and high loading capacity (1320 mg g^{-1}). Furthermore, HST shows more effective bactericidal activity against *E. coli* and *S. aureus* than thymol. In addition, SEM image show that HST indeed had a remarkable inhibitory effect against *E. coli* and *S. aureus* by disrupting the structure of cell membrane. Thus, HST is a promising strategy to facilitate its application as antimicrobial agents.

Acknowledgements

This study was supported by special funding for the development of science and technology of Shanghai Ocean University.

References

[1] Rakkhumkaew N and Pengsuk C 2018 *Food Sci. Biotechnol.* **27** 1201
[2] Friedman M 2017 *J. Agric. Food Chem.* **65** 10406
[3] Jeong E Y, Lee M J and Lee H S 2018 *Food Sci. Biotechnol.* **27** 1541
[4] Orhan-Yanıkan E, da Silva-Janeiro S, Ruiz-Rico M, Jiménez-Belenguer A I, Ayhan K and Barat J M 2019 *Food Control* **101** 29
[5] Amiri P, Shahpiri A, Asadollahi M A, Momenbeik F and Partow S 2016 *Biotechnol. Lett.* **38** 503
[6] Ruiz-Rico M, Pérez-Esteve É, Bernardos A, Sancenón F, Martínez-Máñez R, Marcos M D *et al* 2017 *Food Chem.* **233** 228
[7] Fang C, Al-Suwayeh S and Fang J Y 2012 *Recent Pat. Nanotechnol.* **7** 41
[8] Jin L, Liu X, Bian C, Sheng J, Song Y and Zhu Y 2019 *Chin. Chem. Lett.* **31** 2137

[9] Jin L, Teng J, Hu L, Lan X, Xu Y, Sheng J *et al* 2019 *J. Sci. Food Agric.* **99** 5168
[10] Bilia A R, Guccione C, Isacchi B, Righeschi C, Firenzuoli F and Bergonzi M C 2014 *Evid. Based Complement. Alternat. Med.* **14** Article ID 651593
[11] Asbahani A E, Miladi K, Badri W, Sala M, Addi E H A, Casabianca H *et al* 2015 *Int. J. Pharm.* **483** 220
[12] Kladniew B, Islan G, García de Bravo M, Duran N and Castro G 2017 *Colloid Surf. B Biointerfaces* **154** 123
[13] Quintans-Júnior L, Barreto R, Menezes P, Almeida J R, Viana A, Oliveira R *et al* 2013 *Basic Clin. Pharm. Toxicol.* **113** 167
[14] Xiao Z, Lei D, Zhu G and Niu Y 2015 *J. Polym. Res.* **22** 10
[15] Yang Z, Niu Z, Lu Y, Hu Z and Han C 2003 *Angew. Chem.* **42** 1943
[16] Dai J T, Zhang Y, Li H C, Deng Y H, Elzatahry A A, Alghamdi A *et al* 2017 *Chin. Chem. Lett.* **28** 531
[17] Hu J, Chen M, Fang X and Wu L 2011 *Chem. Soc. Rev.* **40** 5472
[18] Puglia C, Lauro M R, Tirendi G G, Fassari G E, Carbone C, Bonina F *et al* 2017 *Exp. Opin. Drug Deliv.* **14** 755
[19] Zhu Y, Shi J, Shen W, Dong X, Feng J, Ruan M *et al* 2005 *Angew. Chem.* **44** 5083
[20] Li T, Geng T, Md A, Banerjee P and Wang B 2019 *Colloid Surf. B Biointerfaces* **176** 185
[21] Mei X, Chen D, Li N, Xu Q, Ge J, Li H *et al* 2012 *Microporous Mesoporous Mater.* **152** 16
[22] Mishra A, Pandey H, Agarwal V, Ramteke P and Pandey A 2014 *J. Nanopart. Res.* **16** 1
[23] Zea C, Alcántara J, Barranco-García R, Morcillo M and Fuente D 2018 *Nanomaterials* **8** 478
[24] Huo W, Zhang X, Hu Z, Chen Y, Wang Y and Yang J 2018 *J. Am. Ceram. Soc.* **102** 955
[25] Nandiyanto A B D, Kim S G, Iskandar F and Okuyama K 2009 *Microporous Mesoporous Mater.* **120** 447
[26] Rahman Z U, Wei N, Li Z, Sun W and Wang D 2017 *New J. Chem.* **41** 14122
[27] Ulloa P A, Guarda A, Valenzuela X, Rubilar J F and Galotto M J 2017 *Food Sci. Biotechnol.* **26** 1763
[28] Stöber W, Fink A and Bohn E 1968 *J. Colloid Interface Sci.* **26** 62
[29] Bajpai V K, Al-Reza S, Choi U, Lee J and Chul S 2009 *Food Chem. Toxicol.* **47** 1876
[30] Hyldgaard M, Mygind T and Meyer R L 2012 *Front Microbiol.* **3** 12
[31] Marinescu G, Culita D C, Romanitan C, Somacescu S, Ene C D, Marinescu V *et al* 2020 *Appl. Surf. Sci.* **520** 146379
[32] Grumezescu A M, Andronescu E, Ficai A, Grumezescu V, Bleotu C, Saviuc C *et al* 2013 *Curr. Org. Chem.* **17** 1029
[33] Gounani Z, Asadollahi M A, Meyer R L and Arpanaei A 2018 *Int. J. Pharm.* **537** 148
[34] Janatova A, Bernardos A, Smid J, Frankova A, Lhotka M, Kourimská L *et al* 2015 *Ind. Crops Prod.* **67** 216